Published in final edited form as:

Arterioscler Thromb Vasc Biol. 2021 December ; 41(12): 2961–2973. doi:10.1161/ATVBAHA.121.316911.

CircSOD2, a Novel Regulator for Smooth Muscle Proliferation And Neointima Formation

Xiaohan Mei[1,2], **Xiao-Bing Cui**[1], **Yiran Li**[3], **Shi-You Chen**[1,2,4,*]

[1]Departments of Surgery, University of Missouri School of Medicine, Columbia, MO;

[2]Department of Physiology & Pharmacology, University of Georgia, Athens, GA;

[3]Institute of Bioinformatics, University of Georgia, Athens, GA;

[4]Department of Medical Pharmacology & Physiology, University of Missouri School of Medicine, Columbia, MO

Abstract

Objective: Vascular smooth muscle cell (SMC) proliferation contributes to neointima formation following vascular injury. Circular RNA (circRNA), a novel type of non-coding RNA with closed-loop structure, exhibits cell- and tissue-specific expression patterns. However, the role of circRNA in SMC proliferation and neointima formation is largely unknown. The objective of this study is to investigate the role and mechanism of circSOD2 in SMC proliferation and neointima formation.

Approach and Results: CircRNA profiling of human aortic SMCs revealed that platelet-derived growth factor (PDGF)-BB up- and down-regulated numerous circRNAs. Among them, circSOD2, derived from back-splicing event of superoxide dismutase 2, was significantly enriched. Knockdown of circSOD2 by short hairpin RNA (shRNA) blocked PDGF-BB-induced SMC proliferation. Inversely, circSOD2 ectopic expression promoted SMC proliferation. Mechanistically, circSOD2 acted as a sponge for microRNA 206, leading to upregulation of NOTCH3 and NOTCH3 signaling, which regulates cyclin D1 and CDK4/6. *In vivo* studies showed that circSOD2 was induced in neointima SMCs in balloon-injured rat carotid arteries. Importantly, knockdown of circSOD2 attenuated injury-induced neointima formation along with decreased neointimal SMC proliferation.

Conclusions: CircSOD2 is a novel regulator mediating SMC proliferation and neointima formation following vascular injury. Therefore, circSOD2 could be a potential therapeutic target for inhibiting the development of proliferative vascular diseases.

[*]**Corresponding author:** Shi-You Chen, PhD, Department of Surgery, University of Missouri School of Medicine, 1 Hospital Drive, Columbia, MO 65212, scqvd@missouri.edu, Tel: 573-884-0371.

Disclosures: None

Supplemental Materials
Expanded Methods
Online Figures I – XII
Major Resources Table
Data Set (online Table I)
References 51–52

Keywords

Smooth muscle; Proliferation; CircSOD2; Neointima formation; NOTCH3 signaling

Subject codes:

115; 123; 162

Introduction

Vascular injury-induced neointima formation is a complex pathological process and often occurs after percutaneous coronary intervention, bypass surgery, or cardiac transplantation, etc. Neointimal hyperplasia in proliferative vascular diseases remains a significant issue despite numerous pharmacological and mechanical approaches have been advanced in recent years[1]. Smooth muscle cells (SMCs) within the medial layer of the artery wall usually maintain in a quiescent state until they are activated to a proliferative state in response to vascular injuries, such as mechanical stretch, medical dissection, and endothelial denudation, leading to exposure to circulating growth factors or mitogens[1, 2]. SMC proliferation is considered as a crucial step in the development of neointima formation[1]. Thus, investigation of molecular mechanisms responsible for SMC proliferation is vital for achieving a better understanding of the pathogenesis of proliferative vascular disorders.

Transcriptomic studies have revealed that up to 90% human genome is transcribed, but only 1–2% of transcripts encode proteins. Substantial numbers of transcripts are categorized as non-coding RNAs (ncRNAs)[3]. Emerging evidence has shown that ncRNAs are multifunctional regulators associated with many diseases, including developmental, oncological, neurological, cardiovascular, autoimmune, and cutaneous disorders[4–7]. As a novel class of ncRNA, circular RNA (circRNA) has been found to play a potent role in multiple biological processes and exhibit tissue- and disease-specific expression patterns[8]. Unlike linear RNA, circRNA undergoes back-splicing, forming a covalently closed loop structure without 3′ and 5′ ends[9]. Owing to the unique feature, circRNA is speculated to have higher stability and longer half-life than linear RNA due to its resistance to exonuclease degradation and thereby execute exclusive cellular regulatory fuctions[10]. Only a few studies have investigated circRNA roles in vascular diseases. SMC-enriched circ_Lrp6 regulates SMC proliferation and differentiation via mediating miR-145[11]. CircMAP3K5 in SMCs appears to be a master regulator for microRNA (miR)-22-3p/TET2 axis in regulating the neointimal hyperplasia[12].

In this study, we first conducted a circRNA profiling via RNA sequencing (RNA-Seq) of transcripts in control and PDGF-BB-treated human aortic SMCs (HASMCs) and then identified a circRNA candidate derived from the parental gene superoxide dismutase 2 (SOD2). CircSOD2 was significantly upregulated upon PDGF-BB treatment in both *in silico* and *in vitro* expression analyses. Knockdown of circSOD2 by shRNA abolished PDGF-BB-induced HASMC proliferation, whereas ectopic expression of circSOD2 promoted HASMC proliferation. Mechanistically, circSOD2 sponged miR-206, which blocked the

inhibitory effect of miR-206, leading to an elevated NOTCH3 signaling axis and thus increased HASMC proliferation. Importantly, *in vivo* study revealed that knockdown of circSOD2 attenuated injury-induced neointimal formation along with the suppression of SMC proliferation, indicating that circSOD2 is a novel regulator for SMC proliferation and neointima formation.

Materials and Methods

The authors declare that all supporting data are available within the article (and its online supplementary files).

Animals

Male Sprague-Dawley rats weighing 450–500 g were purchased from Charles River Laboratories. All animals were housed under conventional conditions in an animal care facility and received humane care in compliance with the Principles of Laboratory Animal Care formulated by the National Society for Medical Research and the Guide for the Care and Use of Laboratory Animals. Animal surgical procedures were approved by the Institutional Animal Care and Use Committee of the University of Missouri. Sex is a critical biological variable in cardiovascular diseases[13]. Since this is the first report investigating circSOD2 function in vascular diseases, only male animals were used in this study. However, we will investigate if there is a sex-specific role of circSOD2 in neointima formation by including both male and female animals in our future studies.

CircRNA identification and quantification

The RNA-seq raw reads were cleaned and trimmed by Trimmomatic version 0.36[14]. Reads quality was analyzed by FastQC (https://qubeshub.org/resources/fastqc) version 0.11.9. CircRNA candidates were detected by CIRCexplorer2 pipeline version 2.3.0[15]. Briefly, cleaned reads were aligned onto hg19 genome (http://genome.ucsc.edu/) using Tophat2 version 2.1.1[16, 17]. Bam files from alignment were then parsed by CIRCexplorer2 parse module to generate bed files that contained reads information supporting back-splicing junction. Then circRNA annotation was conducted by CIRCexplorer2 annotation module based on annotation files of hg19 genome fetched from the UCSC annotation database. Data merge and processing were performed in R. To avoid infinity values, a pseudo-count of 1 was added to each circRNA read number. The relative expression level of each circRNA was calculated using the formula: SRPBM (Spliced Reads per Billion Mapped Reads) = total number of back-spliced junction reads/the total number of mapped reads*1,000,000,000[18]. Differential expression of circRNAs was estimated using the Limma Linear Models[19]. In pairwise comparisons, circRNAs with $P < 0.01$ and absolute fold change greater than 2 were considered to be differentially expressed. All differentially expressed circRNAs was listed in Online Table I.

Construction of adenoviral vector expressing circSOD2 shRNA

Short hairpin RNAs (shcircSOD2) specifically targeting the back-splicing junctions (BSJ) of human and rat circSOD2 were inserted into pRNAT-H1.1/Adeno vector (Genscript) between MluI and HindIII site. Adenoviral vectors of shcircSOD2 (Ad-shcircSOD2)

were constructed using AdEasy system[20]. Adenoviruses were purified by gradient density ultracentrifugation of cesium chloride followed by dialysis in dialysis buffer (135 mmol/L NaCl, 1mmol/L $MgCl_2$, 10 mmol/L Tris-HCl, pH 7.5, 10% glycerol). Primers for construction of the human and rat circSOD2 shRNAs were listed in Major Resources Table.

Plasmid construction

For circSOD2 expression plasmid (pcircSOD2) construction, full length circSOD2 cDNA was amplified from the HASMC mRNA using Phusion High-Fidelity PCR Master Mix (Thermo Scientific, F531S) and was inserted into a pcDNA3.1(+) CircRNA Mini Vector (a gift from Dr. Jeremy Wilusz[21], Addgene plasmid #, 60648) between Hind III and Xho I restriction site by using In-Fusion HD Cloning reagents (Clonetech, 638910). Residual sequences flanking the full length of circSOD2 on plasmid, which could be mistakenly included into circSOD2 after circularization, were removed by QuikChange II XL Site-Directed Mutagenesis Kit (Agilent, 200521). For luciferase reporter assay, the full length circSOD2 was amplified from the human SMC cDNA pool and was inserted downstream of firefly luciferase cassette in a PGL4.23 vector with minimal promoter at the Xba I site. All vectors were verified by sequencing. The primers amplifying circSOD2, used in mutagenesis and infusion cloning were listed in Major Resources Table.

RNA pull-down assay

RNA pull-down assay was adapted from RNA Antisense Purification protocol with some modifications[22, 23]. We first synthesized anti-circSOD2 probe targeting circSOD2 BSJ and control probes with 10% biotin-UTP (Roche, 11388908910) using *in vitro* transcription kit (Promega, P1300). The primers used in probe synthesis were listed in Major Resources Table. HASMCs at 80–90% confluence on 15-cm culture dishes were fixed with 2% formaldehyde solution at 37°C for 10 mins before being lysed in 200 μl lysis buffer [20 mM HEPES (pH 7.5), 50 mM KCl, 0.5 mM EDTA, 1.5mM $MgCl_2$, 1% (v/v) NP-40, and 0.4% (w/v) sodium deoxycholate (pH 7.5), 0.1% (w/v) N-lauroylsarcosine] containing 40 units/ml RiboLock RNase Inhibitor (Thermo Scientific, EO0384) and 1x protease inhibitors. After 10 mins of incubation on ice, cell lysates were homogenized by passing through a 27-gauge needle 20 times, and then the supernatants were collected by centrifugation at 13,000×g for 20 mins. Cell lysates (200 μl) were added with 800 μl hybridization/wash buffer [20 mM Tris-HCl (pH 7.5), 7 mM EDTA, 3 mM EGTA, 150 mM LiCl, 1% (v/v) NP-40, 0.2% (w/v) N-lauroylsarcosine, 0.1% (w/v) sodium deoxycyolate] supplied with RNase and protease inhibitors, and then was pre-cleared by incubation with 50 μl of Streptavidin Magnetic Beads (NEB, S1420S) at 37°C for 20 mins. Meanwhile, probes (1μg for each probe) were denatured in water at 85°C for 1 min and then immediately transferred to ice. The pre-cleared lysates were incubated with the denatured probes (500 μl each probe) at 37°C for 2 hours with rotation, followed by adding 500 μl pre-washed Streptavidin Magnetic Beads and incubating with rotation for 30 mins. After six times of washing with hybridization/wash buffer, beads were incubated in Proteinase K Digestion Buffer [20 mM Tris-HCl pH 7.5, 10 mM EDTA, 2% N-lauroylsarcosine] supplied with 20 μg/ml of proteinase K at 42 °C for 1 h to digest protein and reverse formaldehyde crosslinks. RNA was purified by using RNA Clean & Concentrator kit (Zymo, R1017) by following the small RNA purification

protocol. Elution from the column was subjected to RT-qPCR analyses. Primers used for miRNA reverse transcription and qPCR were listed in Major Resources Table.

Fluorescent in situ hybridization (FISH)

Biotin-labeled antisense circSOD2 RNA probes and negative control probes derived from eGFP gene were synthesized as described previously[4]. HASMCs grown on coverglasses were firstly washed with cold PBS twice and then fixed with 1% PFA for 30 mins at room temperature, followed by wash with PBS for three times. Permeabilization was performed with 0.5% Triton X-100 in PBS for 10 mins followed by PBS wash for three times. Endogenous biotin was blocked by incubation with 0.05% avidin for 15 mins, followed by incubation with 0.005% biotin for 15 mins to block excessive biotin binding pockets on avidin. Free biotins were removed by washing with PBS for three times. The cells were then incubated with pre-denatured probes in hybridization buffer (10% w/v dextran sulfate, 10% formamide, in 2× SSC, 1 mg/ml fragmented salmon testes DNA) in dark and humid environment at 55 °C for 16 h to allow hybridization. After hybridization, cells were washed with wash buffer (10% formamide in 2× SSC) for 3 times. Finally, cells were incubated with streptavidin-conjugated Alexa-fluor 488 (Invitrogen, S11223) in PBS for 1 hour and counterstained with DAPI. For tissue FISH, biotin-labeled rat antisense circSOD2 ssDNA probe was obtained from Integrated DNA Technologies (IDT, Coralville, Iowa). Vessel segments were harvested and fixed in 4% paraformaldehyde at 4°C for 3 h, transferred to 15% sucrose overnight for cryoprotection. Samples were then embedded in Tissue-Tek O.C.T. compound (EMS, Hatfield, PA). Tissue blocks were frozen in liquid nitrogen, stored at −80°C, and 5-μm thick sections were made. The FISH procedure was similar to cellular FISH, except that the tissue sections were incubated with denaturation buffer (30% formamide in 2x SSC) for 5 hours before hybridization. Probe sequences were listed in Major Resources Table.

Statistical analysis

All statistical analyses were performed using GraphPad Prism software version 8. All cell culture-based experiments were repeated for three or nine times. Normality of the data was assessed using Shapiro-Wilk test and the equality of group variance was assessed using *F*-test. All data are presented as mean±SD. Comparisons between 2 groups were performed using 2-tailed Student *t* test or Mann-Whitney test for normal and non-normally distributed data, respectively. One-way ANOVA was used for comparisons among >2 groups with the Tukey post hoc test. A $p<0.05$ was considered statistically significant.

Results

Bioinformatic Identification and Profiling of CircRNAs in SMCs

SMC proliferation is a crucial step in neointima formation[24], and PDGF-BB is a potent stimulator for SMC proliferation[25]. To identify circRNAs involved in SMC proliferation, we profiled circRNA candidates in vehicle and PDGF-BB-treated HASMCs by sequencing their ribosomal RNA-depleted RNAs (Online Figure I, A–B). Raw reads were mapped to human hg19 genome and processed by CIRCexplorer2 to obtain circRNA candidate information, including genomic position, host gene name, and the number of junction

reads supporting circRNA candidates (Online Figure IA). We then used spliced reads per billion mapped reads (SRPBM) to calculate the relative expression of individual circRNAs. RNA sequencing detected 7,713 circRNAs, in which 323 circRNAs were differentially expressed ($p \leq 0.01$ and fold change ≥ 2) (Figure 1A). Besides, 3,192 circRNAs were not previously identified since they are not present in the most comprehensive circRNA database - circBase (http://www.circbase.org/) (Online Figure IC). Among the 323 differentially expressed circRNAs, 62 were upregulated by PDGF-BB (Figure 1B). It appeared that the PDGF-BB-regulated circRNAs are distributed in various different human genomic loci (Figure 1C). In order to validate the authenticity of circRNAs, we randomly selected eight circRNA candidates and performed RT-PCR using divergent primers to specifically amplify BSJs of the circRNAs on both human genomic DNA and HASMC cDNA. The amplicons were subject to Sanger sequencing to verify the presence of BSJs. As shown in Online Figure II, A–B, all eight circRNAs were endogenously expressed and matched with the RNA-Seq results, suggesting a high fidelity and reliability of the circRNA identification pipeline.

Characterization of PDGF-BB Enriched CircSOD2

Among the differentially expressed circRNAs, circSOD2, derived from host gene SOD2, was highly upregulated in PDGF-BB-treated cells (Figure 1A) and thus was selected for further investigation. CircSOD2 is 462nt long and contains three exons from SOD2 pre-mRNA (Figure 2A). The genomic location of circSOD2 is on the reverse strand of human chromosome 6, starting from 160,103,505 to 160,109,274. By performing the divergent primer amplification and Sanger sequencing of the BSJ amplicon, we confirmed the circSOD2 sequence annotated from the circRNA identification pipeline (Figure 2B). To further validate the authenticity of circSOD2, we performed RNase R digestion using RNA isolated from HASMCs. RNase R is a ribonuclease only digesting linear RNAs while leaving the RNAs with loop structure intact. CircSOD2 showed resistance to RNase R digestion, whereas linear host gene SOD2 and housekeeping gene cyclophilin mRNAs were degraded by RNAase R (Figure 2C). Cellular fractioning followed by RT-qPCR revealed that circSOD2 was largely located in SMC cytoplasm while only a small portion was in the nuclei (Figure 2D). Since RNA-Seq showed that circSOD2 was highly induced by PDGF-BB (Figure 2E), we treated HASMCs with 20 ng/ml PDGF-BB for 0, 12, 24, and 48 hours to validate circSOD2 expression. As shown in Figure 2F, circSOD2 expression was induced by PDGF-BB in a time-dependent manner. RNA-FISH of circSOD2 also showed that circSOD2 was enriched in PDGF-BB-treated HASMCs and mainly located in the cytoplasm (Figure 2G). In addition to SMCs, CircSOD2 was detected in many human tissues, including brain, kidney, heart, skeletal muscle etc., based on the information retrieved from a database circAtlas 2.0 (http://159.226.67.237:8080/new/index.php) (Online Figure III), suggesting that circSOD2 is a ubiquitously expressed circRNA in many tissues and cell types[26].

CircSOD2 Was Required for PDGF-BB-Induced SMC proliferation

To determine whether circSOD2 is involved in HASMC proliferation, we conducted a series of loss and gain-of-function experiments. We first designed two small interfering RNAs (siRNAs) specifically targeting circSOD2 BSJ with different coverages and confirmed

their knockdown efficiency (Online Figure IV, A). CircSOD2 siRNAs did not alter the expression of its parental gene SOD2 (Online Figure IV, B–C). We then constructed an adenoviral vector expressing circSOD2 short hairpin RNA (shRNA) (shcircSOD2) based on the siRNA1 sequence because it showed a better knockdown efficiency. The parental SOD2 level was also unimpacted by shcircSOD2 (Online Figure IV, D–E). In order to determine if circSOD2 is important for SMC proliferation, we tested if circSOD2 knockdown alters the expression of genes regulating cell proliferation in PDGF-BB-treated HASMCs. As shown in Figure 3, A–B, circSOD2 shRNA reversed PDGF-BB-upregulated PCNA expression while increased the expression of $P27^{kip}$, a well-known SMC proliferation inhibitor,[27] that was suppressed by PDGF-BB. Conversely, forced expression of circSOD2 increased PCNA while inhibited $P27^{kip}$ expression (Figure 3, C–D). EDU and CCK8 assays showed that knockdown of circSOD2 decreased PDGF-BB-induced HASMC proliferation (Figure 3, E–G).

Because cell growth relies on cell cycle progression, we hypothesized that circSOD2 might regulate HASMC cell cycle transition. Indeed, knockdown of circSOD2 attenuated PDGF-BB-promoted G1-to-S transition in HASMCs, and thus arrested HASMCs in the G1 phase (Figure 4, A–B). On the other hand, forced expression of circSOD2 promoted G1-to-S phase transition of HASMCs (Online Figure V, A–B). Since G1-to-S phase transition is associated with cyclin-dependent kinases CDK4 and CDK6, which form complexes with D-type cyclins,[28] we tested if circSOD2 regulates the expression of these kinases. As shown in Figure 4, C–D, circSOD2 shRNA inhibited PDGF-BB-induced expression of Cyclin D1, CDK4, and CDK6, but did not affect the expression of Cyclin A and B, suggesting that circSOD2 mediates PDGF-BB-induced SMC cell cycle progression through Cyclin D1, CDK4, and CDK6. These results indicated that circSOD2 is a novel factor regulating SMC proliferation.

CircSOD2 bound miR-206

Since circSOD2 was predominantly expressed in the cytoplasm of HASMCs (Figure 2D and 2G), we hypothesized that circSOD2 might act as a miRNA sponge to regulate gene expression. As a critical element of RNA-induced silencing complex (RISC), Argonaute RISC Catalytic Component 2 (Ago2) binds with miRNA to form a complex to target mRNAs[29]. RNA immunoprecipitation (RIP) assays revealed that circSOD2 bound Ago2 (Figure 5A). circRNA pull-down assay using biotin-labeled circSOD2 BSJ RNA probe followed by RT-qPCR identified three miRNA candidates that potentially bind with circSOD2 (Figure 5B), as predicted by miRanda package[30]. Among these miRNAs, miR-206 was highly enriched by circSOD2 probe (Figure 5B) and showed tentative site for binding to circSOD2 (Figure 5C, upper panel). We thus cloned the circSOD2 linear sequence into pGL4.23 luciferase reporter immediately after the luciferase gene to generate pGL4-circSOD2 reporter vector. Luciferase assays showed that miR-206 mimic significantly decreased the luciferase activity of pGL4-circSOD2 in HASMCs, as compared to the scramble miRNA mimic (Figure 5C), demonstrating that circSOD2 physically bound miR-206. Interestingly, miR-206 expression was significantly decreased in PDGF-BB-treated HASMCs in a time-dependent manner (Online Figure VI, A), and knockdown of circSOD2 significantly increased miR-206 level in vehicle- and especially in PDGF-BB-

treated HASMCs (Online Figure VI, B). These results suggested that circSOD2 could regulate miR-206 level via physical binding.

CircSOD2 Regulates SMC Proliferation via circSOD2-miR-206-NOTCH3 Axis

NOTCH signaling is a vital regulator for SMC differentiation and proliferation. PDGF-BB activates NOTCH3 to promote SMC proliferation through MAP kinase signaling, Hes-related proteins, Cyclin D expression and platelet-derived growth factor receptor-beta (PDGFR-β)[31–33]. Knockdown of circSOD2 in HASMCs significantly reduced PDGF-BB-induced NOTCH3 expression, ERK1/2 phosphorylation, P38 phosphorylation and HEY1 (Figure 6, A–B), suggesting that circSOD2 was essential for NOTCH3 signaling in SMCs. Although PDGFR-β did not respond to PDGF-BB stimulation, knockdown of circSOD2 significantly reduced PDGFR-β expression (Online Figure VII, A–B).

Since miR-206 has been shown to bind NOTCH3 mRNA 3' UTR (Figure 6C, upper panel) and down-regulate NOTCH3 expression in SMCs[34], we speculated that circSOD2 might mediate PDGF-BB-activated NOTCH3 signaling by sponging miR-206. To test this, we performed a miR-206 mimic rescue assay by co-transfecting scramble or miR-206 mimics with control or circSOD2 overexpression plasmid followed by vehicle or PDGF-BB treatment. As shown in Figure 6, C–D, circSOD2 upregulated NOTCH3 and PCNA expression, especially in PDGF-BB-treated cells, but miR-206 mimics alleviated these effects.

To further examine the relationship between circSOD2 and NOTCH3, we applied NOTCH3 siRNA in HASMCs and found NOTCH3 knockdown abolished circSOD2-induced proifertive effect of HASMCs (Online Figure VIII, A–D). Since cyclin D1 has been shown to be a direct target of NOTCH3[35] and its expression was modulated by circSOD2 (Figure 4, C–D), we sought to determine whether circSOD2 affects NOCTH3 interaction with cyclinD1 promoter in HASMCs. ChIP assay showed that knockdown of circSOD2 significantly suppressed NOTCH3 binding to cyclin D1 promoter in a chromatin setting (Online Figure IX, A–B), suggesting that circSOD2 is required for NOTCH3-mediated cyclin D1 gene transcription, in addition to sponging miR-206 to promote NOTCH3 signaling cascade.

Knockdown of CircSOD2 Attenuated Injury-Induced Neointimal Formation

In the normal artery, circSOD2 showed a very low level of expression. However, in a rat carotid balloon injury model, injury significantly induced circSOD2 expression in neointimal SMCs (Figure 7, A–B). Quantitative analyses revealed that circSOD2 was significantly induced as early as three days after the injury, and its expression reached the highest level 7 days and maintained the level (7.8 folds increase) until 14 days post-injury (Online Figure X, A). To determine whether circSOD2 is functionally vital for neointimal formation, we incubated endothelium-denuded rat carotid arteries with control or shcircSOD2 for 20 minutes immediately after the balloon injury in order to transduce circSOD2 shRNA into carotid arterial SMCs. RNA-FISH and RT-qPCR assay confirmed that circSOD2 level was reduced by 70% in the shcircSOD2-treated vessels (Figure 7, A–B and Online Figure X, B). Importantly, knockdown of circSOD2 significantly

attenuated injury-induced neointimal formation (Figure 7, C–D) with significant reductions in neointima area, intima/media ratio, and intima/lumen ratio (Figure 7, E). To determine if circSOD2 regulates neointimal SMC proliferation *in vivo*, we detected PCNA expression in injured arteries. Immunofluorescent staining showed that knockdown of circSOD2 decreased the PCNA+ SMC number by 50% in neointima as compared with the injured arteries transduced with scramble shRNA (Figure 7, F–G).

Additionally, since cell apoptosis and macrophage infiltration are also involved in neointimal formation, we detected if circSOD2 is involved in cell survival or inflammatory response in the injured arteries. As shown in Online Figure XI, A–B, knockdown of circSOD2 enhanced cell apoptosis and suppressed macrophage infiltration in neointima area. However, knockdown of circSOD2 did not impact SMC marker gene expression in cultured HASMCs (Online Figure XII, A–B), suggesthing that circSOD2 may promote injury-induced neointima formation by promoting SMC survival and proliferation as well as macrophage infiltration.

Discussion

CircRNAs have been found to be important players in the development of multiple diseases. Although the expression levels of circRNAs are relatively low compared with mRNAs, the circRNAs have longer average half-life with 24–48 hours[36] compared with the linear mRNAs whose average lifetime is only 4 to 9 hours. Therefore, circRNAs are considered to be very promising regulators to modify gene expression patterns via acting as miRNA sponges, RNA binding protein scaffold, nuclear transcriptional regulator, or peptide/protein translation templates[37]. Our study identified circSOD2 as a novel regulator for SMC proliferation and neointima formation. PDGF-BB treatment increased circSOD2 expression in HASMCs. Although a very low level of circSOD2 expression was observed in normal healthy arterial SMCs, circSOD2 was highly upregulated in the proliferative neointimal SMCs in balloon-injured arteries. Notably, circSOD2 maintained a high level of expression for a relatively long time post-injury, which is likely due to the resistance to exonuclease degradation. Functionally, knockdown of circSOD2 repressed while overexpression of circSOD2 promoted SMC proliferation. Most importantly, circSOD2 knockdown attenuated neointima formation while inhibiting SMC proliferation in injured arteries *in vivo*, indicating that circSOD2 promotes neointima formation by stimulating SMC proliferation.

CircSOD2 regulates SMC proliferation by promoting cell cycle progression. Specifically, circSOD2 appears to be important for G1-to-S phase transition. Knockdown of circSOD2 caused cell cycle arrest at the G1 phase. At the molecular level, circSOD2 inhibits the expression of cyclin-dependent kinase inhibitor $p27^{Kip1}$.CircSOD2 is also essential for PDGF-BB-induced expression of cyclin D1, CDK4 and CDK6, suggesting that circSOD2 may promote cell cycle progression in SMCs by both inhibiting $p27^{Kip1}$ and promoting CDK4/6 expression/activity. CircSOD2 does not affect the expression of cyclin A and B, indicating that circSOD2 mainly regulates the G1-to-S transition, but not other phases.

CircSOD2 regulates cell cycle progression/SMC proliferation by serving as a miR-206 sponge. MiR-206 level has been shown to be critical for SMC proliferation[38], and

miR-206 mimics overrided circSOD2 activity and thus inhibited circSOD2-mediated SMC proliferation. Interestingly, miR-206 expression was negatively correlated with circSOD2 level, indicating that circSOD2 could regulate miR-206 via sponge activity. These results are consistent with other reports showing that circRNAs regulate miRNA expression via physical binding although the underlying mechanisms remain to be determined[12, 39, 40].

In addition to miR-206, miR-150-5p and miR-15a-5p also bind to circSOD2. Several targets have been identified for MiR-150-5p in different cells such as TP53, VEGFA. CXCR4, DLL4, and FZD4. There are also target genes linked to miR-15a-5p including VEGF and WNT3A. Although miR-206, miR-150-5p, and miR-15a-5p were all significantly enriched in the pull-down assay, miR-206 was the most enriched miRNA compared with the other two. Besides, miR-206 is a well-studied miRNA in SMCs[34, 41]. Therefore, we only selected miR-206 for the downstream analyses, which is one of the limitations for this study. Since circRNA can sponge multiple miRNAs to regulate cell behavior[42], and miR-150-5p and miR-15a-5p also modulate cell proliferation, we could study if these two miRNAs also play roles in mediating circSOD2 downstream signaling in the future.

NOTCH signaling pathway is highly conserved and important for vascular development and physiology[33]. Among different NOTCH receptors, NOTCH2 and NOTCH3 play important roles in SMC growth, survival, and cell fate determination[43]. NOTCH2 inhibits PDGF-BB-induced SMC proliferation, whereas NOTCH3 promotes SMC proliferation through MEK/ERK1/2 signaling[32]. CircSOD2 promotes NOTCH3 expression and its downstream signaling because knockdown of circSOD2 decreased NOTCH3 expression and the activation of many NOTCH3 downstream modulators, such as p38, ERK1/2, and HEY1. CircSOD2 appears to promote NOTCH3 downstream signaling and thus cyclin D1 expression and G1-to-S transition by suppressing miR-206 inhibitory activity[44, 45], which is consistent with previous studies showing that miR-206 is a potent inhibitor for NOTCH3 expression[31, 46].

Interestingly, knockdown of circSOD2 inhibits PDGFR-β expression, suggesting that circSOD2 positively regulates PDGF signaling. CircSOD2 is likely to promote PDGFR-β expression through increasing NOTCH3 signaling. NOTCH3 has been shown to promote PDGFR-β expression in SMCs[47]. Thus, circSOD2 may mediate a feed-forward mechanism to augment the interaction between PDGF and NOTCH3 signaling in SMCs, i.e., PDGF-BB induces circSOD2, which enhances NOTCH3 signaling by sponging miR206. The enhanced NOTCH3 in turn promotes PDGFR-β expression, which further boosts PDGF signaling. Since PDGF-BB activates both PDGFR-α and PDGFR-β, it is unclear if there is a compensatory effect by PDGFR-α when PDGFR-β is inhibited by circSOD2 shRNA, which could be studied in the future.

As a newly-identified RNA molecule, circSOD2 function remains largely unknown. Recent studies have shown that circSOD2 is upregulated in human esophageal cancer, hepatocellular carcinoma, and papillary thyroid carcinoma[48, 49]. Knockdown of circSOD2 impairs liver cancer cell growth[50]. Moreover, circSOD2 is expressed in multiple human tissues (Online Figure III) and is upregulated in different cells/tissues/plasma of human patients as revealed by next-generation RNA sequencing or microarray analyses (https://

www.ncbi.nlm.nih.gov/geo/, Project# PRJNA639542, PRJNA389189, PRJNA381880 and PRJNA721442). Our study demonstrates a new role for circSOD2 in SMC proliferation and intimal hyperplasia. Therefore, circSOD2 could be a potential biomarker for proliferation-related diseases.

One of the limitations in this study is the lack of circSOD2 genetically modified mouse model. It appears that circSOD2 not only promotes SMC proliferation, but also regulates cell survival and macrophage infiltration. However, the specific roles of circSOD2 derived from these cells *in vivo* are still unclear, which could be investigated in the future when the circSOD2 genetically modified mouse becomes available. Nevertheless, this study has revealed a novel mechanism underlying SMC proliferation and injury-induced neointima formation. The mechanism involves circSOD2 promotion of NOTCH3/CyclinD1/CDK4/6 axis via inhibition of miR-206 in SMCs. Therefore, targeting circSOD2/miR-206/NOTCH3 axis may be a promising strategy to hinder injury-induced neointima formation in proliferative vascular diseases.

Supplementary Material

Refer to Web version on PubMed Central for supplementary material.

Sources of Funding

This work was supported by grants from National Institutes of Health (HL119053, HL135854, and HL147313, R01HL117247 to S.-Y.C.).

Abbreviations:

PDGF-BB	Platelet-derived growth factor-BB
SMC	Smooth muscle cell
CDK	Cyclin-dependent kinase
FISH	Fluorescent in situ hybridization
RIP	RNA immunoprecipitation
ncRNA	Noncoding RNA
circRNA	circular RNA
SOD2	Superoxide Dismutase 2
BSJ	Back splicing junction

Reference:

1. Marx SO, Totary-Jain H & Marks AR Vascular smooth muscle cell proliferation in restenosis. Circ Cardiovasc Interv 4, 104–111 (2011). [PubMed: 21325199]
2. Kalavakunta JK, Gangula S & Gupta V In-stent ulceration: an unusual pathology. Case Rep Cardiol 2014, 893143 (2014). [PubMed: 24826314]

3. Consortium EP The ENCODE (ENCyclopedia Of DNA Elements) Project. Science 306, 636–640 (2004). [PubMed: 15499007]
4. Tang R, Zhang G, Wang YC, Mei X & Chen SY The long non-coding RNA GAS5 regulates transforming growth factor beta (TGF-beta)-induced smooth muscle cell differentiation via RNA Smad-binding elements. J Biol Chem 292, 14270–14278 (2017). [PubMed: 28659340]
5. Tang R et al. LncRNA GAS5 regulates vascular smooth muscle cell cycle arrest and apoptosis via p53 pathway. Biochim Biophys Acta Mol Basis Dis 1865, 2516–2525 (2019). [PubMed: 31167125]
6. Tang R et al. LncRNA GAS5 attenuates fibroblast activation through inhibiting Smad3 signaling. Am J Physiol Cell Physiol 319, C105–C115 (2020). [PubMed: 32374674]
7. Esteller M Non-coding RNAs in human disease. Nat Rev Genet 12, 861–874 (2011). [PubMed: 22094949]
8. Jeck WR et al. Circular RNAs are abundant, conserved, and associated with ALU repeats. RNA 19, 141–157 (2013). [PubMed: 23249747]
9. Zhang XO et al. Complementary sequence-mediated exon circularization. Cell 159, 134–147 (2014). [PubMed: 25242744]
10. Zhang Y et al. The Biogenesis of Nascent Circular RNAs. Cell Rep 15, 611–624 (2016). [PubMed: 27068474]
11. Hall IF et al. Circ_Lrp6, a Circular RNA Enriched in Vascular Smooth Muscle Cells, Acts as a Sponge Regulating miRNA-145 Function. Circ Res 124, 498–510 (2019). [PubMed: 30582454]
12. Zeng Z et al. Circular RNA CircMAP3K5 Acts as a MicroRNA-22-3p Sponge to Promote Resolution of Intimal Hyperplasia via TET2-Mediated SMC Differentiation. Circulation (2020).
13. Robinet P et al. Consideration of Sex Differences in Design and Reporting of Experimental Arterial Pathology Studies-Statement From ATVB Council. Arterioscler Thromb Vasc Biol 38, 292–303 (2018). [PubMed: 29301789]
14. Bolger AM, Lohse M & Usadel B Trimmomatic: a flexible trimmer for Illumina sequence data. Bioinformatics 30, 2114–2120 (2014). [PubMed: 24695404]
15. Zhang XO et al. Diverse alternative back-splicing and alternative splicing landscape of circular RNAs. Genome Res 26, 1277–1287 (2016). [PubMed: 27365365]
16. Trapnell C, Pachter L & Salzberg SL TopHat: discovering splice junctions with RNA-Seq. Bioinformatics 25, 1105–1111 (2009). [PubMed: 19289445]
17. Kim D & Salzberg SL TopHat-Fusion: an algorithm for discovery of novel fusion transcripts. Genome Biol 12, R72 (2011). [PubMed: 21835007]
18. Tan WL et al. A landscape of circular RNA expression in the human heart. Cardiovasc Res 113, 298–309 (2017). [PubMed: 28082450]
19. Ritchie ME et al. limma powers differential expression analyses for RNA-sequencing and microarray studies. Nucleic Acids Res 43, e47 (2015). [PubMed: 25605792]
20. Luo J et al. A protocol for rapid generation of recombinant adenoviruses using the AdEasy system. Nat Protoc 2, 1236–1247 (2007). [PubMed: 17546019]
21. Liang D & Wilusz JE Short intronic repeat sequences facilitate circular RNA production. Genes Dev 28, 2233–2247 (2014). [PubMed: 25281217]
22. Engreitz JM et al. RNA-RNA interactions enable specific targeting of noncoding RNAs to nascent Pre-mRNAs and chromatin sites. Cell 159, 188–199 (2014). [PubMed: 25259926]
23. Engreitz JM et al. The Xist lncRNA exploits three-dimensional genome architecture to spread across the X chromosome. Science 341, 1237973 (2013). [PubMed: 23828888]
24. Pauletto P, Sartore S & Pessina AC Smooth-muscle-cell proliferation and differentiation in neointima formation and vascular restenosis. Clin Sci (Lond) 87, 467–479 (1994). [PubMed: 7874832]
25. George SJ, Williams A & Newby AC An essential role for platelet-derived growth factor in neointima formation in human saphenous vein in vitro. Atherosclerosis 120, 227–240 (1996). [PubMed: 8645364]
26. Wu W, Ji P & Zhao F CircAtlas: an integrated resource of one million highly accurate circular RNAs from 1070 vertebrate transcriptomes. Genome Biol 21, 101 (2020). [PubMed: 32345360]

27. Marra DE, Simoncini T & Liao JK Inhibition of vascular smooth muscle cell proliferation by sodium salicylate mediated by upregulation of p21(Waf1) and p27(Kip1). Circulation 102, 2124–2130 (2000). [PubMed: 11044431]
28. Topacio BR et al. Cyclin D-Cdk4,6 Drives Cell-Cycle Progression via the Retinoblastoma Protein's C-Terminal Helix. Mol Cell 74, 758–770 e754 (2019). [PubMed: 30982746]
29. Winter J, Jung S, Keller S, Gregory RI & Diederichs S Many roads to maturity: microRNA biogenesis pathways and their regulation. Nat Cell Biol 11, 228–234 (2009). [PubMed: 19255566]
30. Enright AJ et al. MicroRNA targets in Drosophila. Genome Biol 5, R1 (2003). [PubMed: 14709173]
31. Morris HE, Neves KB, Montezano AC, MacLean MR & Touyz RM Notch3 signalling and vascular remodelling in pulmonary arterial hypertension. Clin Sci (Lond) 133, 2481–2498 (2019). [PubMed: 31868216]
32. Baeten JT & Lilly B Differential Regulation of NOTCH2 and NOTCH3 Contribute to Their Unique Functions in Vascular Smooth Muscle Cells. J Biol Chem 290, 16226–16237 (2015). [PubMed: 25957400]
33. Fouillade C, Monet-Lepretre M, Baron-Menguy C & Joutel A Notch signalling in smooth muscle cells during development and disease. Cardiovasc Res 95, 138–146 (2012). [PubMed: 22266753]
34. Jalali S et al. Mir-206 regulates pulmonary artery smooth muscle cell proliferation and differentiation. PLoS One 7, e46808 (2012). [PubMed: 23071643]
35. Cohen B et al. Cyclin D1 is a direct target of JAG1-mediated Notch signaling in breast cancer. Breast Cancer Res Treat 123, 113–124 (2010). [PubMed: 19915977]
36. Enuka Y et al. Circular RNAs are long-lived and display only minimal early alterations in response to a growth factor. Nucleic Acids Res 44, 1370–1383 (2016). [PubMed: 26657629]
37. Li X, Yang L & Chen LL The Biogenesis, Functions, and Challenges of Circular RNAs. Mol Cell 71, 428–442 (2018). [PubMed: 30057200]
38. Xing T et al. Upregulation of microRNA-206 induces apoptosis of vascular smooth muscle cells and decreases risk of atherosclerosis through modulating FOXP1. Exp Ther Med 14, 4097–4103 (2017). [PubMed: 29104627]
39. Chen X et al. Circular RNA circHIPK3 modulates autophagy via MIR124-3p-STAT3-PRKAA/AMPKalpha signaling in STK11 mutant lung cancer. Autophagy 16, 659–671 (2020). [PubMed: 31232177]
40. Zhang J et al. Circular RNA_LARP4 inhibits cell proliferation and invasion of gastric cancer by sponging miR-424–5p and regulating LATS1 expression. Mol Cancer 16, 151 (2017). [PubMed: 28893265]
41. Li H et al. Myocardin inhibited the gap protein connexin 43 via promoted miR-206 to regulate vascular smooth muscle cell phenotypic switch. Gene 616, 22–30 (2017). [PubMed: 28342807]
42. Zheng Q et al. Circular RNA profiling reveals an abundant circHIPK3 that regulates cell growth by sponging multiple miRNAs. Nat Commun 7, 11215 (2016). [PubMed: 27050392]
43. Gridley T Notch signaling in vascular development and physiology. Development 134, 2709–2718 (2007). [PubMed: 17611219]
44. Ravenhall C, Guida E, Harris T, Koutsoubos V & Stewart A The importance of ERK activity in the regulation of cyclin D1 levels and DNA synthesis in human cultured airway smooth muscle. Br J Pharmacol 131, 17–28 (2000). [PubMed: 10960064]
45. Meloche S & Pouyssegur J The ERK1/2 mitogen-activated protein kinase pathway as a master regulator of the G1- to S-phase transition. Oncogene 26, 3227–3239 (2007). [PubMed: 17496918]
46. Song G, Zhang Y & Wang L MicroRNA-206 targets notch3, activates apoptosis, and inhibits tumor cell migration and focus formation. J Biol Chem 284, 31921–31927 (2009). [PubMed: 19723635]
47. Jin S et al. Notch signaling regulates platelet-derived growth factor receptor-beta expression in vascular smooth muscle cells. Circ Res 102, 1483–1491 (2008). [PubMed: 18483410]
48. Shi P et al. Profiles of differentially expressed circRNAs in esophageal and breast cancer. Cancer Manag Res 10, 2207–2221 (2018). [PubMed: 30087579]
49. Ren H et al. Profile and clinical implication of circular RNAs in human papillary thyroid carcinoma. PeerJ 6, e5363 (2018). [PubMed: 30123704]

50. Zhao Z et al. CircSOD2 induced epigenetic alteration drives hepatocellular carcinoma progression through activating JAK2/STAT3 signaling pathway. J Exp Clin Cancer Res 39, 259 (2020). [PubMed: 33234142]

51. Shi N, Li CX, Cui XB, Tomarev SI & Chen SY Olfactomedin 2 Regulates Smooth Muscle Phenotypic Modulation and Vascular Remodeling Through Mediating Runt-Related Transcription Factor 2 Binding to Serum Response Factor. Arterioscler Thromb Vasc Biol 37, 446–454 (2017). [PubMed: 28062493]

52. Schneider CA, Rasband WS & Eliceiri KW NIH Image to ImageJ: 25 years of image analysis. Nat Methods 9, 671–675 (2012). [PubMed: 22930834]

Highlights:

1. circSOD2 is upregulated in SMCs by PDGF-BB and vascular injury.
2. circSOD2 promotes SMC cell cycle progression and proliferation.
3. circSOD2 promotes NOTCH3 signaling by sponging miR-206.
4. circSOD2 is essential for injury-induced neointima formation.

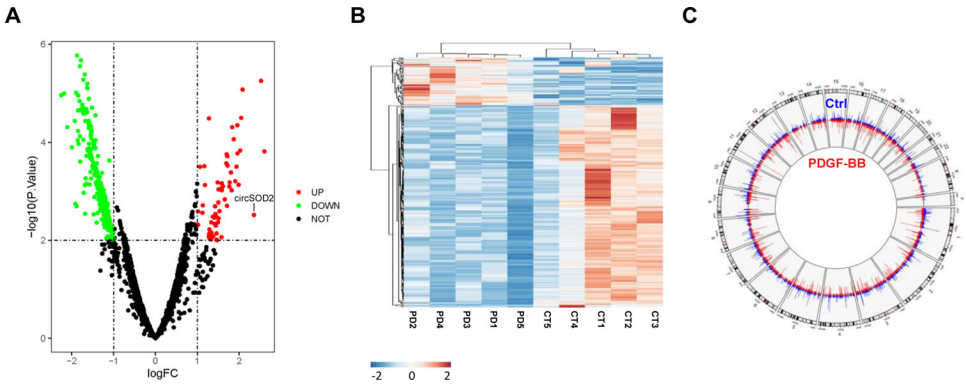

Figure 1. CircRNA expression profile in HASMCs.

HASMCs (<6 passages) were treated with vehicle (Ctrl) or PDGF-BB (20ng/ml) for 48h. RNAseq was conducted to identify circRNAs. **A**, Volcano plot of all identified circRNAs. Red and green dots indicate up-regulated and down-regulated circRNAs with statistical significance, respectively. The cutoff is fold change > 2 with *p*-value < 0.01 (PDGF-BB vs. Ctrl). CircSOD2 is denoted. **B**, Hierarchical clustering and heatmap visualizing the levels of differentially expressed circRNAs. **C**, Circos plot of circRNA distributions on human chromosomes.

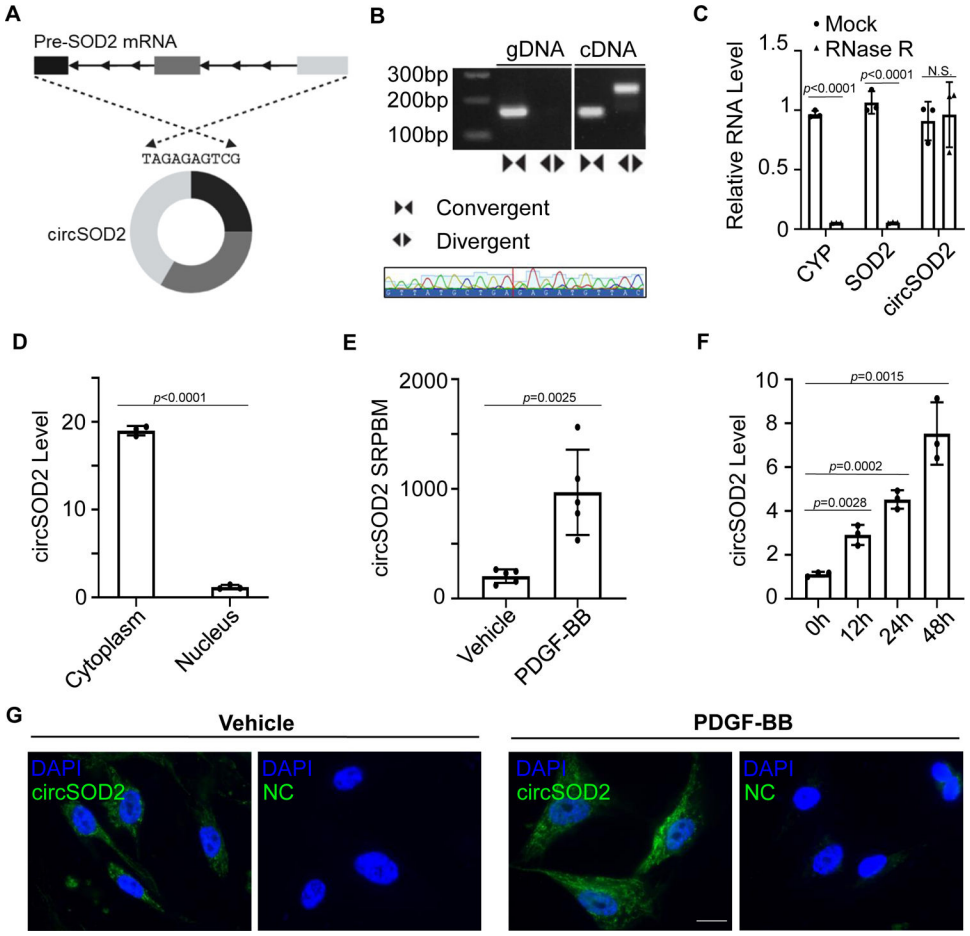

Figure 2. CircSOD2 was upregulated in SMCs by PDGF-BB.

A, Diagram of circSOD2 formation. CircSOD2 was derived from SOD2 pre-mRNA via back-splicing. The region of back-splicing junction is shown. **B**, Divergent primers only amplified circSOD2 in cDNA, but not the genomic DNA (gDNA) (upper panel). Sanger sequencing confirmed the head-to-tail junction (lower panel). Red solid line indicates the back-splicing junction site. **C**, Cyclophilin (CYP) and SOD2 linear RNAs, but not circSOD2, were digested by RNase R, as detected by RT-qPCR (n=3). N.S.: not significant. **D**, CircSOD2 was mainly located in cytoplasm of HASMCs. Cytoplasmic and nuclear RNAs of HASMCs were isolated, and CircSOD2 was assessed by RT-qPCR. The expression was normalized to CYP (n=3). **E**, Spliced reads per billion mapped reads (SRPBM) of circSOD2 from RNAseq data was upregulated by PDGF-BB (20 ng/mL) (n=5). **F**, CircSOD2 was time-dependently induced by PDGF-BB (20 ng/mL) as assessed by RT-qPCR. The expression was normalized to CYP (n=3). **G**, In situ hybridization for circSOD2 in vehicle- or PDGF-BB-treated HASMCs. circSOD2 was detected by biotin-labeled anti-circSOD2 probe (green). Nuclei stained by DAPI (bule). Random probe served as negative control (NC). Bar: 10 μm.

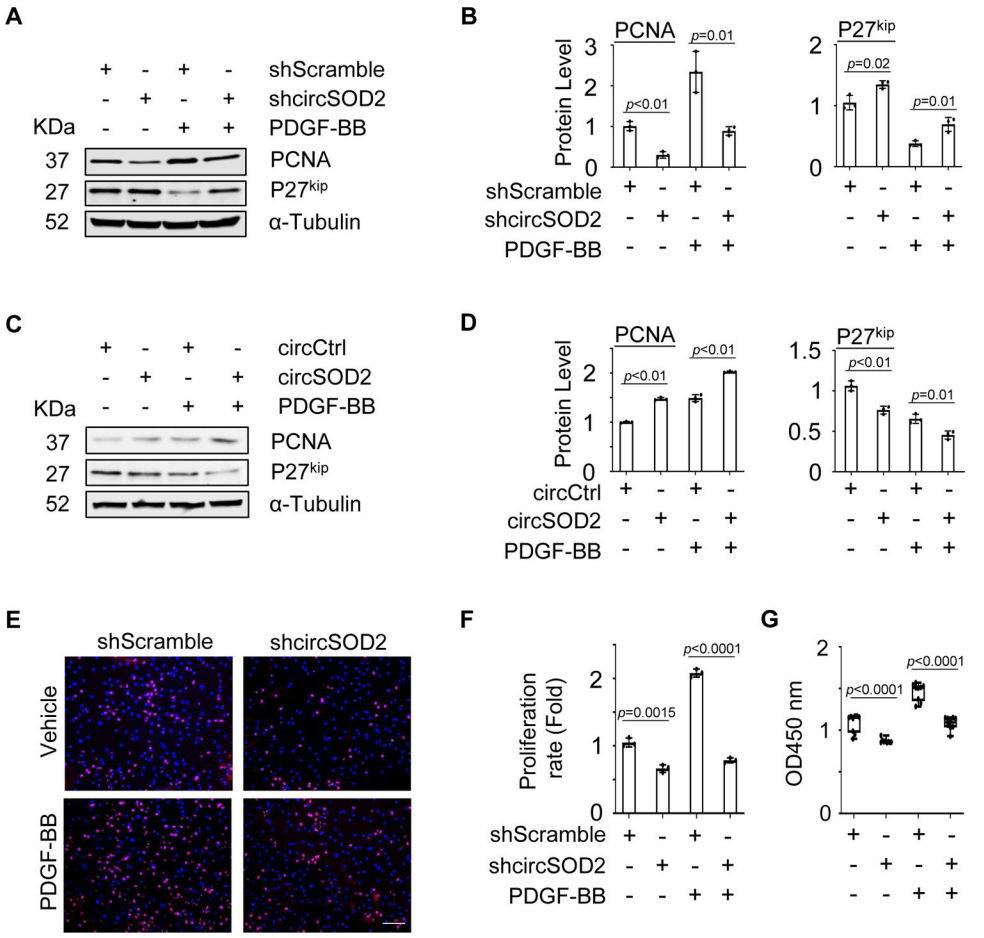

Figure 3. Knockdown of circSOD2 inhibited SMC proliferation.

A, ShRNA knockdown of circSOD2 (shcircSOD2) reversed PDGF-BB-altered PCNA and p27^{kip} expression. HASMCs were tranceduced with scramble (shScramble) or circSOD2 shRNA (shcircSOD2) for 16 h followed by treated with vehicle (−) or PDGF-BB for 48 hours. **B**, Quantification of PCNA and p27^{kip} protein level shown in A by normalizing to α-Tubulin (n=3). **C**, Forced expression of circSOD2 (circSOD2) promoted PCNA while suppressed p27^{kip} expression regulated by PDGF-BB. **D**, Quantification of PCNA and p27^{kip} protein level shown in C by normalizing to α-Tubulin (n=3). **E**, Knockdown of circSOD2 inhibited HASMC proliferation as measured by EdU assay. Bar: 100 μm. **F**, Quantification of EdU-positive cells shown in E (n=3). **G**, Knockdown of circSOD2 inhibited HASMC proliferation as measured by CCK8 assay (n=9).

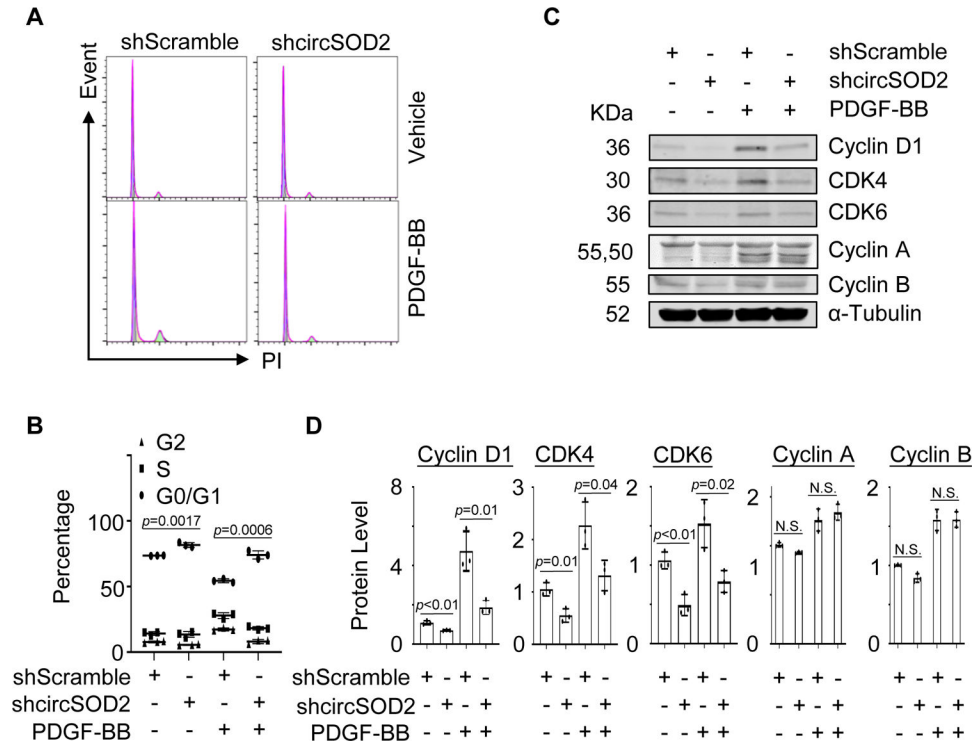

Figure 4. CircSOD2 mediated SMC proliferation via cyclinD1- and CKD4/6-regulated G0/G1 progression.

HASMCs were tranceduced with Scramble (shScramble) or circSOD2 shRNA (shcircSOD2) for 16 hours followed by treatment with vehicle or PDGF-BB for 48 hours. **A**, Knockdown of circSOD2 (shcircSOD2) caused HASMC cell cycle arrest as assessed by Flow cytometry with propidium iodide (PI) staining. **B**, Cell cycle distribution shown in A (n=3). **C**, Knockdown of circSOD2 inhibited Cyclin D1 and CKD4/6 protein expression but had no effect on the expression of Cyclin A and Cyclin B. **D**, Quantification of protein expression shown in C by normalizing to α-Tubulin level (n=3). N.S.: not siginificant.

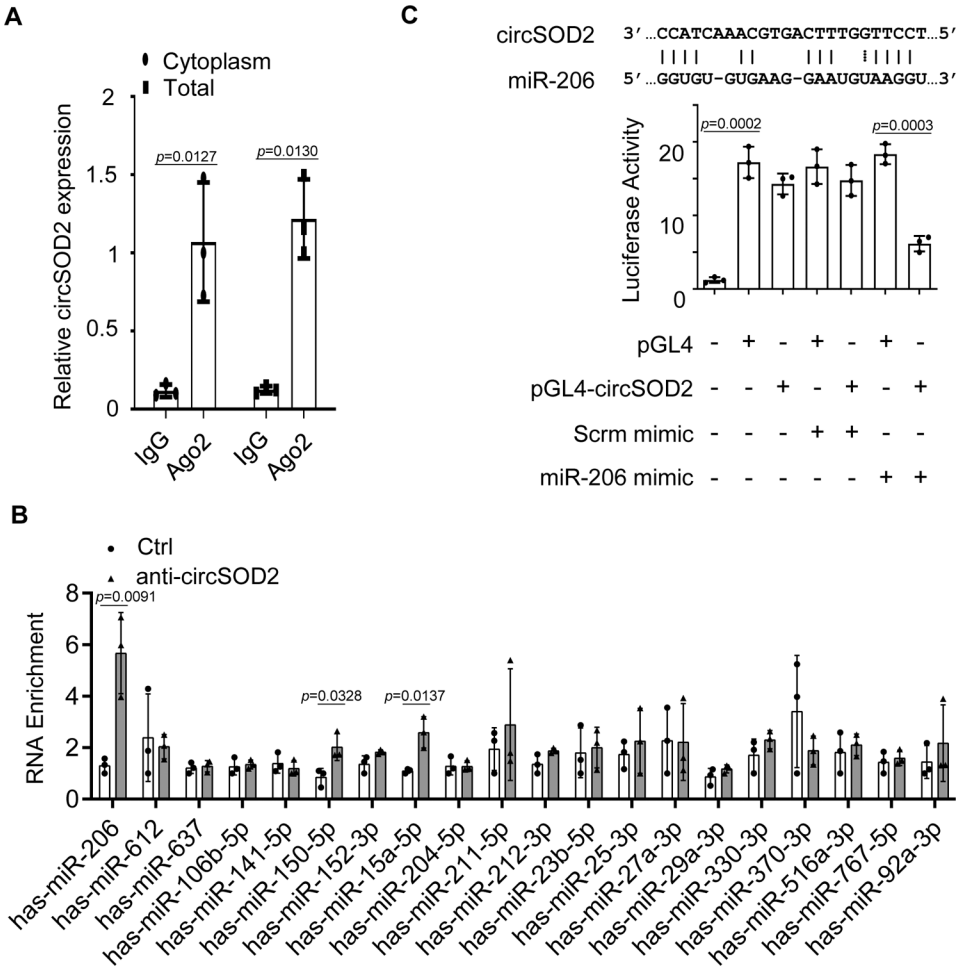

Figure 5. CircSOD2 sponged miRNA-206.

A, HASMC cytoplasmic and total cellular protein fractions were isolated and immunoprecipitated (IP) using Ago2 or IgG antibody. CircSOD2 was detected by RT-qPCR (n = 3). **B**, CircSOD2-interacting molecules was pulled down by biotin-labeled antisense circSOD2 probe. Potential circSOD2-binding microRNAs (miRNA) were screened by RT-qPCR. The expression was normalized to U6 (n=3). **C**, CircSOD2 sponging miRNA-206 was detected by luciferase assay. HASMCs were co-transfected pGL4 luciferase plasmid or pGL4-circSOD2 (containing circSOD2 sequence after luc2P gene) with scramble (Scrm) or miR-206 Mimics. Luciferase activity was detected 48 h after the transfection (n=3). Putative miR-206 binding sites on circSOD2 transcript was shown on the top of the panel. Lower panel.

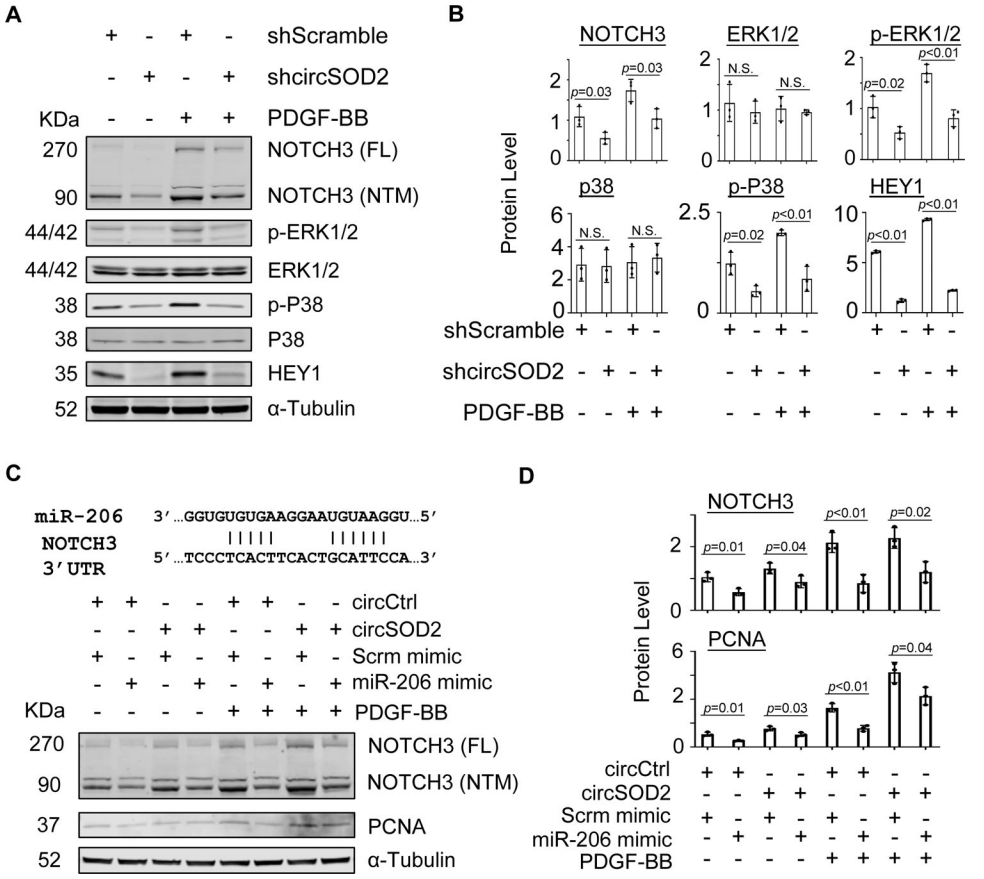

Figure 6. CircSOD2 mediated PDGF-BB-induced SMC proliferation and NOTCH3 expression via sponging miR-206.

A, Knockdown of circSOD2 attenuated PDGF-BB-enhanced NOTCH3 signaling. HASMCs were tranceduced with scramble (shScramble) or circSOD2 shRNA (shcircSOD2) for 16 hours followed by treatment with vehicle or PDGF-BB for 48 hours. NOTCH3 expression and cleavage, ERK1/2 and p38 expression and phosphorylation, as well as HEY1 expression were detected by Western blot. FL: Full length; NTM: NOTCH3 transmembrane domain. **B**, Quantification of protein levels shown in A by normalizing to α-Tubulin (n=3), N.S.: not siginificant. **C**, CircSOD2 mediated NOCTH3 expression via inhibiting miR206 activity. Upper panel: putative miR-206 binding sites on NOTCH3 mRNA3' UTR. Lower panel: control circRNA (circCtrl) or circSOD2 overexpression plasmid were co-transfected into HASMCs with scramble (Scrm mimic) or miR-206 Mimics followed by vehicle or PDGF-BB treatment. NOTCH3 (FL and NTM) and PCNA protein levels were detected by Western blot. **D**, Quantification of protein levels shown in C by normalizing to α-Tubulin (n=3).

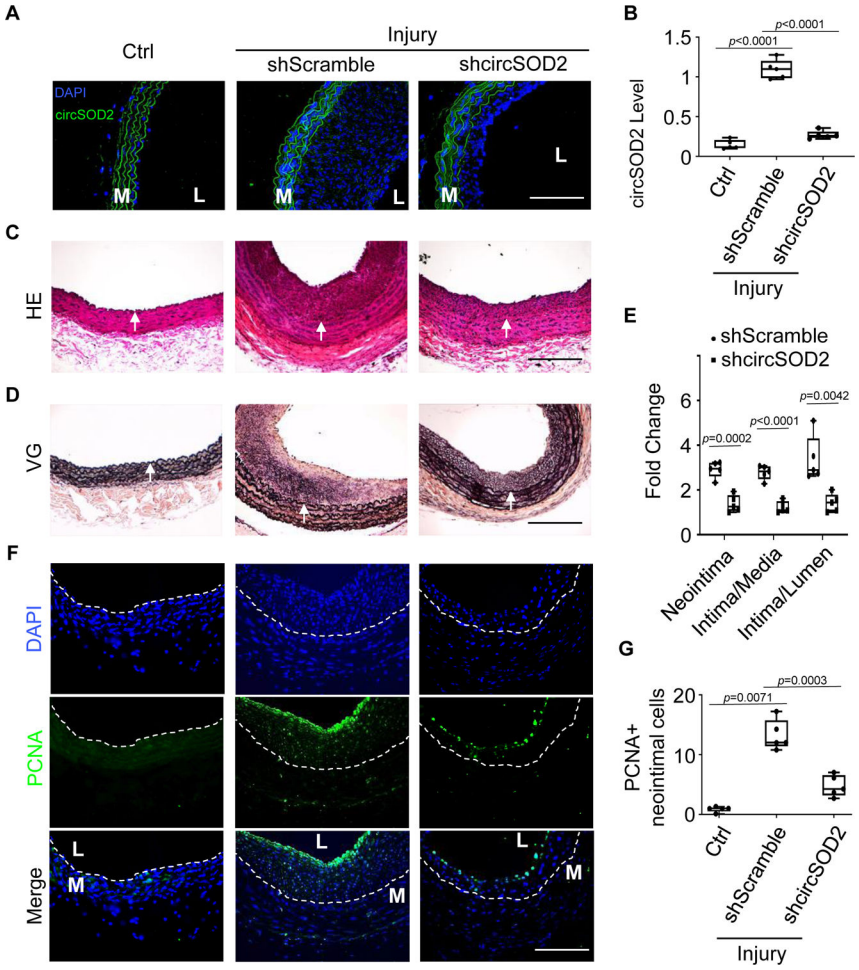

Figure 7. Knockdown of circSOD2 attenuated injury-induced neointima formation *in vivo*.

A, circSOD2 shRNA (shcircSOD2) efficiently reduced circSOD2 level that was upregulated in injured rat carotid arteries. circSOD2 levels in control (Ctrl) or injured arteries (for 14 days) were detected by RNA-FISH. M: media; L: lumen; Bar: 100 μm. **B**, shcircSOD2 knockdown efficiency was confirmed by RT-qPCR with the RNAs extracted from control or injured rat carotid arteries. CircSOD2 levels were normalized to cyclophilin (n=5). **C-D**, Knockdown of circSOD2 by shcircSOD2 blocked injury-induced neointima formation, as shown by H&E (C) and Elastica van Gieson (VG) staining (D). **E**, Quantification of the neointima area, intima/media, and intima/lumen ratio (n=5). **F**, Knockdown of circSOD2 reduced PCNA-positive cell numbers in balloon-injured arteries. Inner elastic lamina was indicated by white dash line. Bar: 100 μm. **G**, Quantification of PCNA-positive neointimal cells shown in F from sections of 5 individual rat arteries (n=5).